Validating CloudSat-CPR retrievals for the estimation of snow accumulation in the Canadian Arctic

by

Fraser Dennis Murray King

A thesis
presented to the University of Waterloo
in fulfillment of the
thesis requirement for the degree of
Masters of Science
in
Geography

Waterloo, Ontario, Canada, 2019

AUTHOR'S DECLARATION

This thesis consists of material all of which I authored or co-authored: see Statement of Contributions included in the thesis. This is a true copy of the thesis, including any required final revisions, as accepted by my examiners.

I understand that my thesis may be made electronically available to the public.

Statement of Contributions

This thesis contains my manuscript journal article submission investigating the ability for CloudSat to accurately measure snow accumulation throughout the Canadian Arctic. This work is ready for submission to the *Journal of Geophysical Research*. The research presented here is the result of a collaborative partnership between myself, my advisor Dr. Chris Fletcher, as well as colleagues from Environment and Climate Change Canada: Dr. Chris Derksen and Dr. Lawrence Mudryk, who have provided insightful advice and guidance in this endeavour. Editing, style and science comments have been provided by Dr. Chris Fletcher throughout the development of this document, with my contributions to this work being the creation of the original draft along with subsequent edited versions.

Abstract

Snow is a critical contributor to our global water and energy budget, with profound impacts for water resource availability, snow albedo feedback and flooding in cold regions. The vast size and remote nature of the Arctic present serious logistical and financial challenges to measuring snow over extended time periods. Satellite observations provided by the Cloud Profiling Radar (CPR) instrument—installed on the NASA satellite CloudSat—allow the retrieval of snowfall rates in high latitude regions, which have been used to estimate surface snow accumulation. In this study, a validation of CloudSat-derived terrestrial snow estimates is presented at four Environment and Climate Change Canada (ECCC) weather stations situated in the Arctic for the common period 2007-2015. Comparisons of monthly climatological snow accumulation show mean biases of less than 1.5 mm SWE annually. Monthly time series exhibit correlations above 0.5 and RMSE below 10 mm SWE at the two highest latitude stations (Eureka and Resolute Bay) with correlations falling below 0.5 south of 70° N. CloudSat was also found to underestimate annual mean snow accumulation at the majority of sites, suggesting a potential negative bias in CloudSat's snowfall estimates, or underestimation related to sampling. These results imply that CloudSat can provide reliable estimates of snow accumulation across similar high latitude regions above 70° N. Accurate space-based snowfall measurements provide new important observational perspectives of Arctic snow accumulation, which is a critical region for environmental monitoring in an era of global change.

Acknowledgements

I would like to thank my parents Geoff and Shelley as well as my sister Kelsey for supporting me during my time in this program by continually providing me with the motivation and inspiration to push through daily challenges. I would also like to thank my advisor Dr. Chris Fletcher who has assisted me every step of the way with targeted direction, honest feedback and by continually sharing his passion for research. The additional advice I received from other members of the science community (Dr. Chris Derksen, Dr. Lawrence Mudryk and Dr. Richard Kelly) has proven to be an invaluable source of information throughout this process. I would also like to extend a big thank you to my lab-mates, roommates and other friends/family for listening to me talk about snow for hours on end; your patience has not gone unnoticed or unappreciated. Finally, I would like to thank my dog Riley, without whom this research would not have been possible.

Table of Contents

List of Tables

List of Figures

Chapter 1

Introduction

1.1 Background

Snow plays a critical role in contributing to our global water and energy budget (Déry and Brown, 2007; Brutel-Vuilmet et al., 2013). Changes to snow accumulation impact global water resource availability, drought and flood frequencies as well as snow cover extent, all of which are rapidly changing due to the effects of Arctic amplification (Hou et al., 2014; Vavrus, 2007; Peacock, 2012; Danco et al., 2016). Recent literature has shown that due to shifting global temperatures, the Arctic is one of the locations seeing the most pronounced changes and fastest overall warming (Serreze and Barry, 2011). Temperature changes have altered atmospheric moisture distributions which has led to increased Arctic precipitation by up to 4% annually, causing increased accumulation during cold periods and reductions during the summer (Dietz et al., 2012). Model estimates have also noted decreases in

the total number of snow cover days across the majority of the Arctic by between 10-20%, along with decreases in snow cover extent by up to 18% by 2050 (Callaghan et al., 2011). However, there are uncertainties associated with these estimates, especially over the Arctic due in part to the limited availability of observational constraints throughout this region with previous studies showing model ensemble estimate standard deviations of snow accumulation by up to 50% (Mudryk et al., 2015; Callaghan et al., 2011). Fig. 1.1 illustrates the differences between two multimodel mean estimates of SWE trends over the 1981-2005 historical period for CMIP5 (Fig 1.1.a) and CanESM (Fig 1.1.b) (Kushner et al., 2018). Understanding how snow is changing at these high latitude locations will allow us to better prepare for and mitigate against the issues we expect to encounter as global temperatures continue to rise.

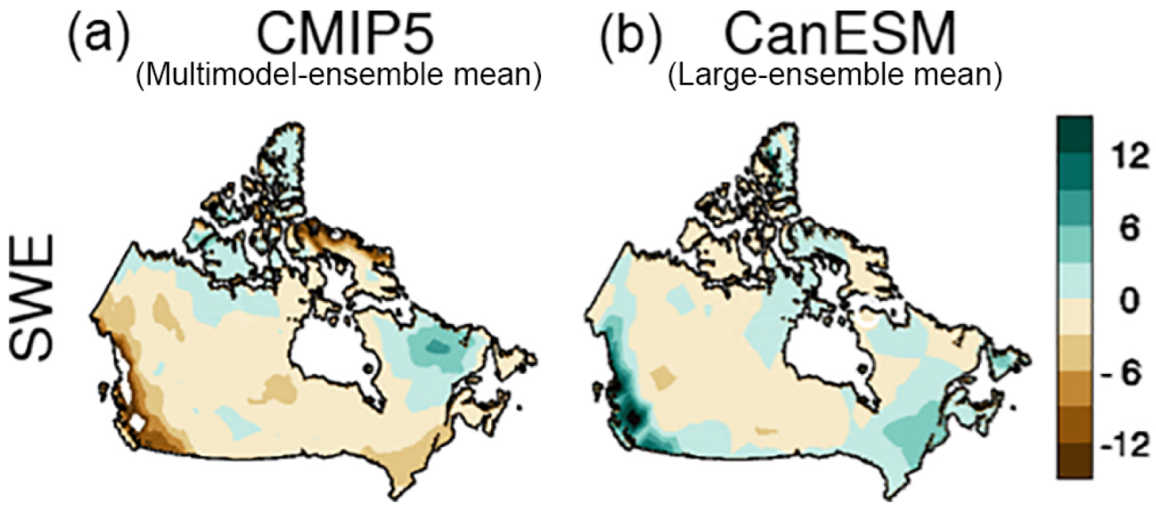

Figure 1.1: (a) 1981-2005 CMIP5 multimodel mean SWE trends over Canada and (b) the corresponding large-ensemble SWE trend means from CanESM (Kushner et al., 2018).

One important quantity for tracking changes in accumulation is snow water equivalent (SWE). SWE is the total amount of liquid water contained within a snowpack that would be produced if the snowpack was to be instantly and completely melted (Doesken and Robinson, 2009). SWE is more formally defined as the product of snowpack depth and snowpack density (with units in mm or kg/m^2), and this quantity is primarily controlled by the surrounding temperature and snowfall availability in the region (Brown and Mote, 2009). SWE displays complex responses to the changes in temperature and precipitation we are experiencing under a warming global climate, and characterizing these changes is of critical importance for deriving accurate and robust predictions in future climate feedbacks (Risnen, 2008).

Measuring SWE by hand is often a time consuming and expensive task, and therefore one common method for obtaining observational measurements is to use automated monitoring instruments to record changes in accumulated SWE. Multiple iterations of automatic weighing gauges like the Geonor or Pluvio series instruments have been actively used across Canada since 2006, providing high temporal resolution measurements of snow accumulation across previously difficult to monitor locations (Mekis et al., 2018). However, when we consider areas above 70° N throughout the Canadian Arctic Archipelago (CAA), this entire region hosts only approximately 1% of all of Canada's active reporting surface weather stations (as shown in Fig. 1.2). Furthermore, due to the vast size of the Arctic, these stations are sparsely distributed and there are considerable observational gaps left between them.

Reanalysis can offer another perspective towards filling these gaps and reducing uncertainty by combining observational records with model estimates of SWE (as described in

section 1.2.2) (Rienecker et al., 2011a; Dee et al., 2011). Products like the Arctic System Reanalysis (ASR) use a combination of assimilated observational station data and numerical model estimates to provide an optimized, low error estimate of SWE through the use of a dynamical model and evolving system states (UCAR/NCAR, 2017). However, since these estimates rely on the availability of input observational data, fewer observations lead to increases in associated uncertainty within the reanalysis system output estimates of SWE due to the additional degrees of freedom introduced as contributions from inherent model biases (Dee and Uppala, 2009). To help combat this uncertainty, one popular method has been to use an ensemble approach (similar to techniques commonly used in weather and climate modelling) where multiple reanalysis products, model outputs and observational datasets are aggregated to help correct for individual product biases and uncertainties (Mudryk et al., 2015). One such blended dataset is the Blended-4 (B4) product which is examined in this report.

The Arctic is one of the most sensitive locations to the effects of climate change. Yet due to its vast size and remote nature, there remain considerable observational gaps when using current methods to derive estimates of SWE. Given the uncertainty and diversity of in situ and reanalysis-based estimates, in this thesis we investigate an alternative approach to estimating accumulated SWE: the Cloud Profiling Radar (CPR) instrument installed onboard the NASA satellite CloudSat.

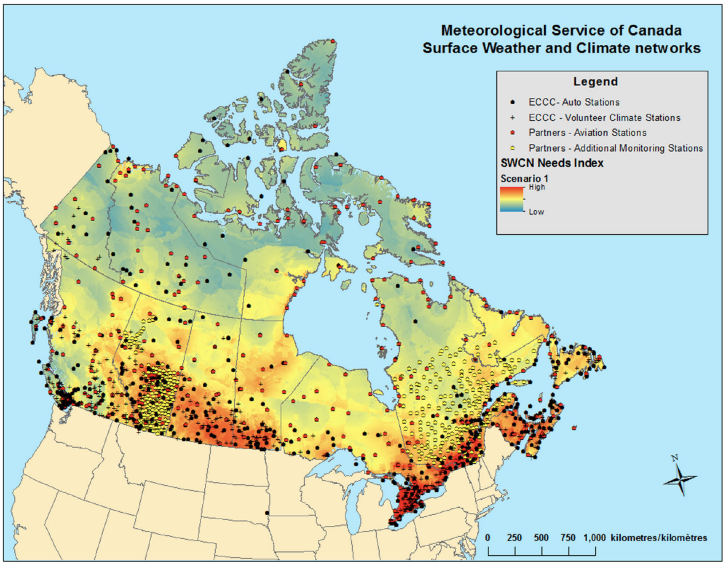

Figure 1.2: Map displaying the location and type of all operational surface weather stations in Canada (Mekis et al., 2018).

1.2 Methods for Measuring Snow Accumulation

1.2.1 In Situ Measurements

One of the longest continuous sources of snow accumulation observations comes from in situ weather station records. The instruments used in obtaining these measurements have undergone many iterations throughout the years, evolving from manual tools requiring constant human supervision, to automatic systems that can run nearly autonomously over prolonged time periods. Two common tools used across North America for measuring changes in accumulated SWE include the Federal Snow Sampler (FSS), and snow pillow (Doesken and Robinson, 2009). The FSS is a portable, manual hand measurement tool equipped with a set of tubes that are used to extract snow core samples from a snowpack

(Beaumont and Work, 1963). The cores are taken at a single point location and the SWE estimates are averaged between each of the cores to provide a more accurate and robust estimate of density throughout the snowpack (Doesken and Robinson, 2009). This technique can provide density information in difficult to reach locations due to the portable nature of the instrument, however it only provides instantaneous snapshots in time at a single point location, and requires the transportation of a trained individual to potentially remote locations.

The snow pillow is another widely used snow accumulation measurement instrument that provides point density measurements of accumulation like the FSS, however it can record measurements autonomously over the course of the entire snow season (Doesken and Robinson, 2009). Snow pillows operate in a similar manner to weighing scales, and estimate snow accumulation by measuring changes in the weight of the snow that is accumulating or melting directly above the device (Marks et al., 2018). Although the observational changes in accumulation have been shown in previous work to generally display high accuracy, snow pillow estimates can often be biased by processes like snow bridging where the snowpack above the gauge partially melts and refreezes, creating a layer of ice which can then support some of the weight of newly fallen snow (Steiner et al., 2018).

More recent techniques for obtaining in situ measurements of SWE involve the use of automatic systems like the Geonor (200B) or Pluvio (PLUVIO1, PLUVIO2) series weighing gauges. Once installed, these devices can provide continual data records of accumulation with minimal human oversight (Mekis et al., 2018). Fig. 1.3 displays a timeline of snow measurement instrument usage periods, describing when each instrument came into widespread use across North America. These automated weighing gauges operate by col-

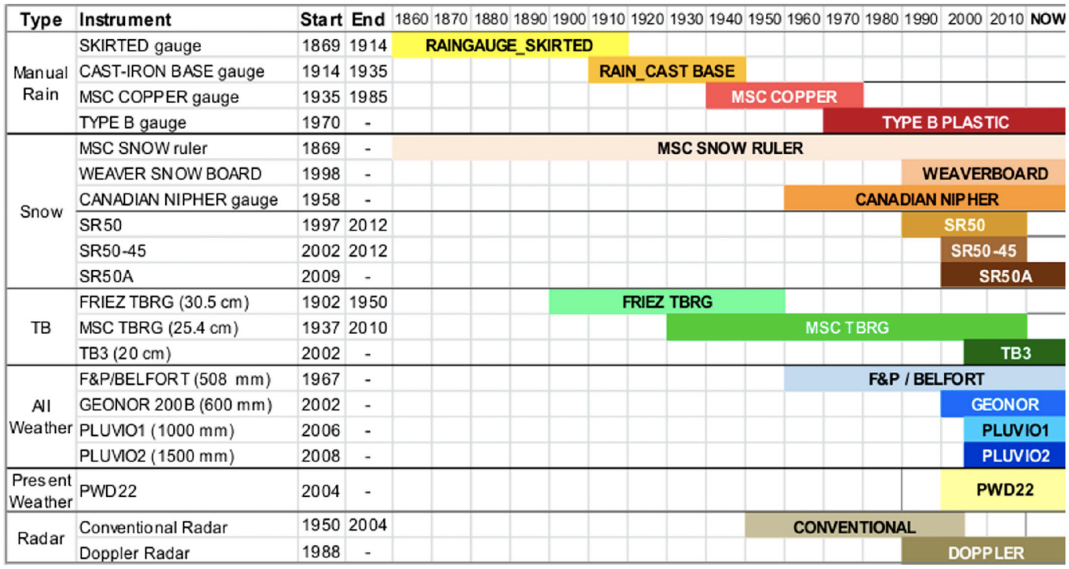

Figure 1.3: Timeline of the periods where each weather observing instrument was commonly used by ECCC across Canada (Mekis et al., 2018).

lecting falling snow into a specialized bucket containing a mixture of water and antifreeze from an opening on the roof of the device (Fountain et al., 2009). This liquid mixture combined with a surface layer of oil, causes snow particles to instantly melt and prevents them from evaporating back into the atmosphere (Smith, 2009). These measurements of accumulation are then recorded by the instrument and remotely transmitted back to the underlying weather network.

Although we can obtain observational records of accumulation using these techniques, their measurements contain uncertainties that must also be considered. Automatic gauges have been shown to often underestimate snowfall accumulation during periods of high winds due to undercatchment problems where snow particles are moving with a high enough velocity to completely avoid capture by the device (Kochendorfer et al., 2017). Shielding

instruments like the Nipher or Alter shields can help to somewhat reduce the impact of this undercatchment issue (as seen in the comparisons of Fig. 1.4), however the problem continues to persist even with a shield once wind speeds reach approximately 10 km hr^{-1} (Doesken and Robinson, 2009). Snowfall can also be blocked from entering instrument orifices from ice formation along the device's openings, or from snow capping that occurs when large snow drifts fully envelope the device (Colli et al., 2015).

In this study, we examine in situ station observations from four separate ECCC weather stations positioned throughout the CAA. These stations are equipped with ground station precipitation weighing gauges (Geonor T-200B) which provide daily estimates of snow accumulation in mm SWE. Uncertainty introduced from snow catchment issues coupled with periods of missing data where no measurements are reported by the station may lead to a potential negative bias in the station data measurements which we consider when performing the analysis.

1.2.2 Reanalysis Systems

Reanalysis systems can offer another perspective towards Arctic snow accumulation by interpolating between gaps in station observations. Reanalysis systems operate by using observational records from external data sources like ground-based stations or satellites to constrain a priori estimates of accumulation generated by a Bayesian numerical forecasting model to estimate evolving system states (Takala et al., 2011). The steps for linking observational records with model estimates differ depending on the data assimilation methods being used in the system (Parker, 2016). These assimilation methods are optimization al-

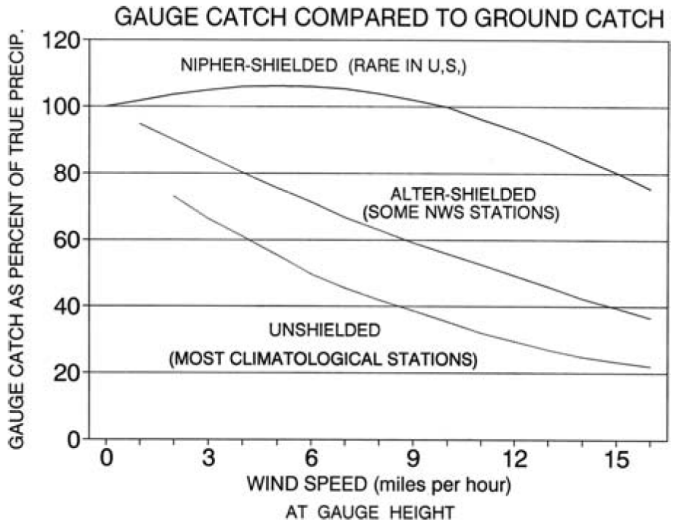

Figure 1.4: Snow core measurements of SWE compared to automatic weighing gauges using different shielding techniques under changing wind-speed intensities (Doesken and Robinson, 2009).

gorithms that use interpolation techniques to minimize the error between what is observed and what is estimated by the forecasting model (Rienecker et al., 2011a). The resulting estimate is the best fit (lowest overall error) for each system state at each time step, and the result is then fed into the following iteration of the algorithm to generate the next system state (Lorenc, 1986). These techniques have been used to great effect when estimating surface parameters like precipitation throughout the Arctic in previous literature, with monthly correlations above 0.75 between station observations and reanalysis products like ERA-Interim (Lindsay et al., 2014).

There are challenges to using reanalysis products throughout the Arctic, due to the limited number of available observations in this region. Since reanalysis systems rely on observations to constrain a numerical model, the fewer available observations, the greater

the uncertainty associated with the system's estimates (Derksen and Brown, 2012). These uncertainties are more pronounced across landscapes that are more difficult to model and observe, such as Arctic regions (which comprise the study area of this report). These regional uncertainties are highlighted in Fig. 1.5 for an ensemble comparison of five separate gridded SWE products, by displaying differences in their multi-dataset mean of snow water mass (SWM) across various land types. SWM is spatially aggregated SWE over a defined region which is then converted to mass using the density of pure water. The comparisons in Fig. 1.5 are performed using the Blended-5 (B5) gridded SWE product which was developed by Mudryk et al. (2015) and includes estimates of SWE from GLDAS-2 (G2), ERA-Interim/Land (E), GlobSnow (G), Crocus (C) and MERRA (M). The anomaly contributions from the multi-dataset mean of the five gridded products included in the Blended-5 dataset are depicted in the shaded regions of Fig. 1.5 for each season across North America (NA), Europe (EU) and the Northern Hemisphere (NH), and we note that the largest anomaly contributors come from alpine and arctic land types. Furthermore, a recent study by Broxton et al. (2016b) suggests that global reanalysis and land data assimilation products often underestimate SWE when compared to high resolution observation-based snow products due to excessive snow ablation occurring when temperatures in the region are fluctuating near 0° C.

In this study we examine two separate reanalysis systems along with a blended product and compare their estimates of snow accumulation (mm SWE) to those recorded by CloudSat. The blended product used in this thesis, is the Blended-4 dataset which is composed of a "blend" or average of four other gridded SWE datasets: CROCUS, GlobSnow, MERRA-2 and Ross Brown's Simple Snow Models (SSM) (Mudryk et al., 2015; Brown and Brasnett,

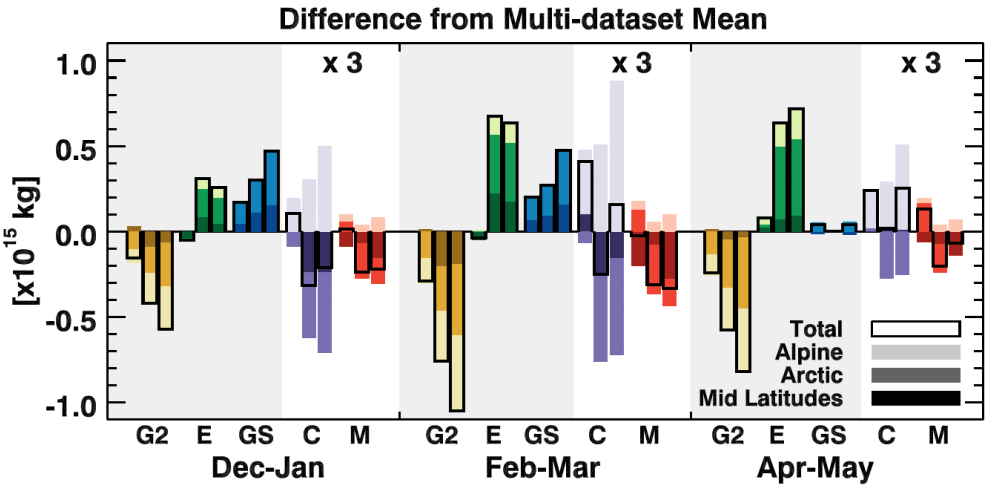

Figure 1.5: Differences in the multi-dataset mean of SWM, with each dataset represented by a different color, over three seasons, for NA, EU and NH with the shaded areas showing the anomaly contributions of different land types (total differences outlined in black) (Mudryk et al., 2015).

2010). This is a different product to the Blended-5 gridded dataset described previously in this section, as it includes a different combination of gridded components which are blended for similar purposes. The Blended-4 product is used here instead of Blended-5 due to its longer overlapping time series with the available CloudSat data record. Although the Blended-4 and Blended-5 products both include SWE estimates from GlobSnow, and Crocus, the remaining datasets in each blended product differ. Since these datasets are produced using different snow models, assimilation schemes and assimilated observations, the resulting Arctic SWE estimates between each product will vary. However, issues related to the poorly constrained nature of the Arctic persist across both datasets, and the blending technique described by Mudryk et al. (2015) has been shown to be a useful method for reducing individual product biases and variability across these regions. The remaining two

reanalysis products included in this comparison are the Arctic System Reanalysis Version 1 (ASRV1) and the Arctic System Reanalysis Version 2 (ASRV2) (Bromwich et al., 2012; UCAR/NCAR, 2017) which use optimized versions of the Polar Weather Forecast Model, in combination with the High Resolution Land Data Assimilation System (HRLDAS) to provide a comprehensive regional climate representation of SWE throughout the Arctic (Bromwich et al., 2012).

1.2.3 Space-Based Remote Sensing

A third perspective for gathering measurements of snowfall over these remote regions, is to use space-based remote sensing techniques. Through the use of specialized satellite instruments, we are able to scan areas of the Earth that are typically difficult or expensive to visit and measure by hand. These observations can be derived from a variety of techniques including active and passive microwave products, airborne LIDAR, hyper-spectral imaging and aerial photography (Dietz et al., 2012). For the purposes of this report, we will analyze the abilities of one satellite in the estimation of snow accumulation: CloudSat, and the active CPR system installed onboard.

CloudSat was launched in 2006 by NASA as part of a program for providing high resolution information about the interior structures of clouds (Kulie et al., 2010). The CPR is a high power 94 GHz (W-band) nadir-facing, active radar instrument with 125 240 meter vertical resolution bins which cover the bottom 30 km of the atmosphere (Tanelli et al., 2008). The instrument itself is sensitive to atmospheric hydrometeors by measuring the power backscattered from interior cloud particles (Marchand et al., 2008). Using this

backscatter information, a radar reflectivity estimate can be generated (Z) which describes interior cloud properties (Kulie and Bennartz, 2009). The detectable signal range required by CloudSat using this frequency lies between ±29 DBz, which makes the instrument highly sensitive to light intensity snowfall (Milani et al., 2018). Additionally, due to the nature of CloudSat's WRS-2 sun-synchronous orbital range of 81° N/S, it produces a high frequency of overpasses at high latitude locations like the Arctic (Fig. 1.6) and in turn, an increased number of observational CPR records that can be used in the estimation of snowfall accumulation throughout the region (Hiley et al., 2010).

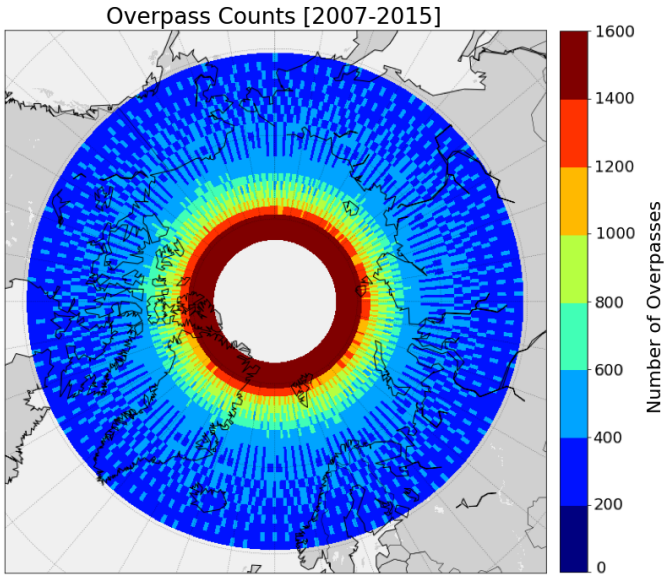

Figure 1.6: A 1° grid of CloudSat overpass count totals from 60° N to 81° N spanning 2007-2015.

Assumptions about the physical and spectral properties of snow particles allow us to use the power backscatter information received by the CPR on CloudSat when it encounters a cloud to infer estimates of atmospheric snowfall rates (Wood et al., 2014). Spectral radar

scattering and reflectivity properties of atmospheric snowfall are closely related to physical snow properties like grain size, shape and particle distribution, along with assumptions about snow composition (purity), density information, ice content and temperature (Dietz et al., 2012). When we consider the radar frequencies used by CloudSat and other active cloud radars, scattering from precipitation-sized particles do not necessarily follow the Rayleigh scattering approximation which can lead to potentially significant attenuation from hydrometeor interference during strong precipitation events (Bucholtz, 1995; Wood et al., 2014). Mie theory has also been used in previous literature to derive single scattering properties of atmospheric hydrometeors and their relationship with radar attenuation (Marzano et al., 2003). These studies suggest that multiple scattering effects are present in space-borne retrievals from instruments like the CPR, when atmospheric conditions allow for the presence of large quantities of high-density ice particles, due to single scattering albedo effects along with the hydrometeor extinction properties of have ice grains (Battaglia et al., 2007). These attenuation issues are potential sources of additional uncertainty in CloudSat snowfall rate estimates, which contribute to retrieval measurement error in the optimal estimation algorithm as described in Wood et al. (2014) for deriving CloudSat's 2C-SNOW-PROFILE.

There are additional uncertainties that must also be considered when using radar backscatter to extract atmospheric snowfall rate estimates of SWE. Radar attenuation is an issue where very intense precipitation events lead to a high amount of between-particle scattering which prevents the backscatter signal from reaching the instrument onboard CloudSat (Haynes et al., 2009). Previous work by Hudak et al. (2008) has shown that this can occur with CPR measurements when the precipitation intensity reaches lev-

els of 5 mm/hr or more. There is also some uncertainty associated with the individual retrieval snowfall rates from CloudSat with a study by Duffy and Bennartz (2018) suggesting additional Bayesian uncertainties upwards of 200% in the derived surface snowfall rate estimates, that arise due to additional a priori model assumptions related to retrieved precipitation state, fallspeed and cloud particle distributions. While other remote sensing techniques exist from projects like NASA's Global Precipitation Measurement (GPM) mission, which could be used as an additional snowfall perspective in this thesis, GPM's orbital coverage has a very limited area of overlap with our region of interest in the Arctic ($\pm 65^{\circ}$ latitude) along with a much shorter overlapping data record (2014-2019) to compare against (Matsui et al., 2013). GPM may however be another useful perspective into atmospheric snowfall rates when performing comparisons at locations further south.

Despite these uncertainties, CloudSat estimates have been used in previous studies to extract surface snow accumulation estimates over similar high latitude locations (Hiley et al., 2010; Milani et al., 2018; Palerme et al., 2017). A CloudSat overpass is composed of a set of spatially averaged snowfall measurements (with a 1.7 km by 1.3 km ground footprint) that are collected when passing near a station. One challenge we encounter when comparing this data to the station observations is finding the appropriate spatio-temporal scales for obtaining a large enough sample of individual CloudSat measurements to accurately represent what is being reported at the station below.

The aggregation of CloudSat overpasses within a predefined spatial grid box has been shown in these studies to be an appropriate technique for performing comparisons between gridded CloudSat retrievals and point station data. Fig. 1.7 shows high correlations and low RMSE between a CloudSat 200 km grid box and point station measurements at Resolute

Bay for one year of SWE data in a study by Hiley et al. (2010). Additional studies by Boening et al. (2012) and Palerme et al. (2017) have shown that CloudSat estimates of snowfall over Antarctica agree well with estimates from the European Centre for Medium-Range Weather Forecasts (ECMWF) product ERA-Interim (August 2006 - April 2011), with a total difference in mean annual snowfall rates of less than 10 mm SWE (171 mm SWE for CloudSat and 163 mm SWE for ERA-Interim) (Fig. 1.8). However, a comparison between CloudSat and in situ observations over the full CloudSat data record has not yet been completed across the Canadian Arctic to my knowledge. We build on the work of these previous studies by using similar overpass gridding techniques in a comparison between CloudSat, station data and reanalysis output across the CAA over (2007-2015), to evaluate CloudSat's general performance throughout this region.

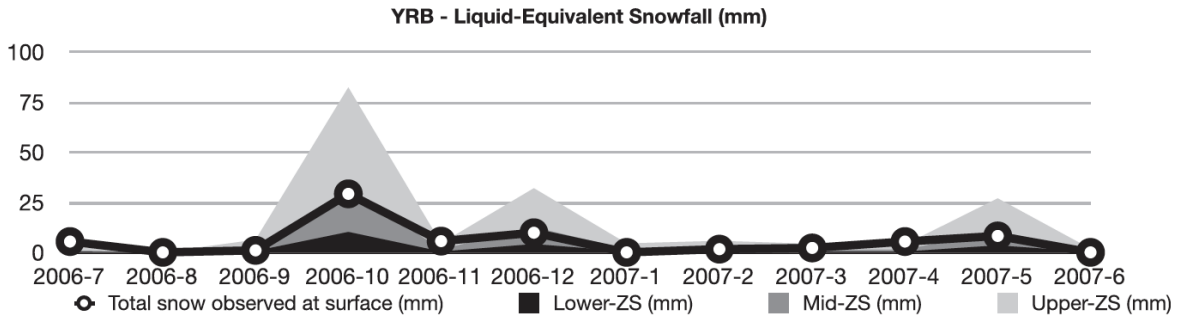

Figure 1.7: Total accumulated SWE for Resolute Bay using three snow-reflectivity relationships (lower, mid and upper) along with the corresponding observed surface stations measurements over one year from 2006-2007 (Hiley et al., 2010).

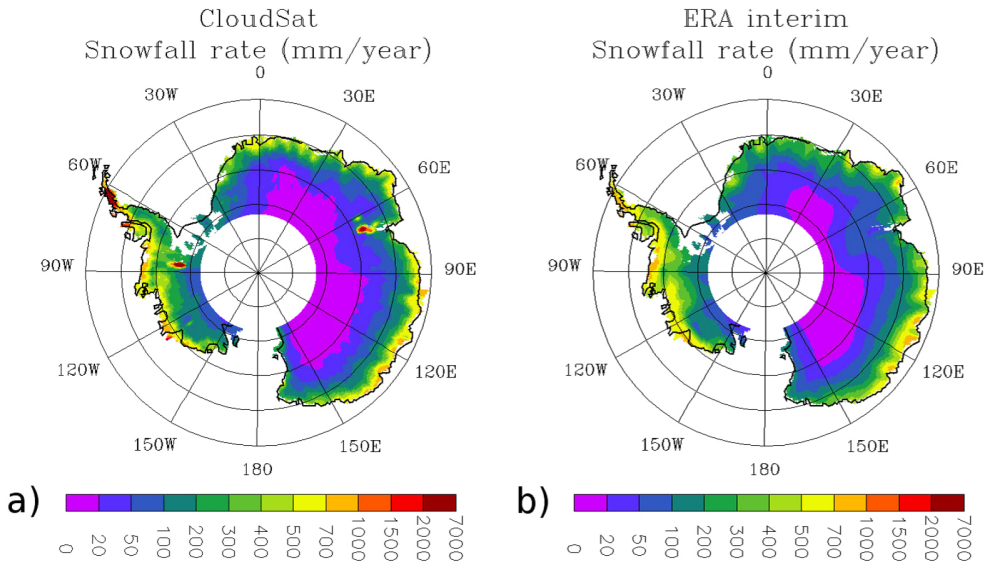

Figure 1.8: Comparison of the mean annual snowfall rates for Antarctica from (a) CloudSat and (b) ERA-Interim over four years (2006-2011) (Palerme et al., 2017).

1.3 Research Objectives

The primary goal of my research is to examine whether CloudSat is an appropriate tool for providing high quality estimates of snow accumulation throughout the Canadian Arctic. To perform this validation, we adopt the validation criteria defined in Hiley et al. (2010) and Palerme et al. (2014), who concluded that temporal correlations above $r = 0.5$, and RMSE below 10 mm of SWE, represent good agreement between CloudSat estimates and ground-truth observations. These criteria are important as they allow us to asses whether CloudSat is capable of capturing the general seasonality of accumulation present at each station throughout the year. Additionally, RMSE of this magnitude is a useful metric for assessing month-to-month variability in CloudSat's estimates of SWE accumulation at

each station, and allows us to identify locations and periods which exhibit high uncertainty in our analysis. Differences in annual mean accumulation rates of approximately 10 mm SWE have also been described as displaying good agreement with low variability in comparisons between CloudSat and reanalysis across Antarctica (Palerme et al., 2014). Additional comparisons between CloudSat and in situ performed in Greenland by Bennartz et al. (2019), have shown what is described as good agreement with monthly correlations above $r = 0.5$ (Fig. 1.9). Building on the results of previous literature, I will perform a validation of CloudSat-CPR observations against measurements from four ECCC weather stations and three gridded SWE products throughout the Canadian Arctic. This thesis will investigate whether through the careful construction of snowfall rate estimates from CloudSat, we can derive an estimate of accumulation that displays strong agreement with station observations, and therefore show that CloudSat provides new insights into snow accumulation throughout other high latitude locations.

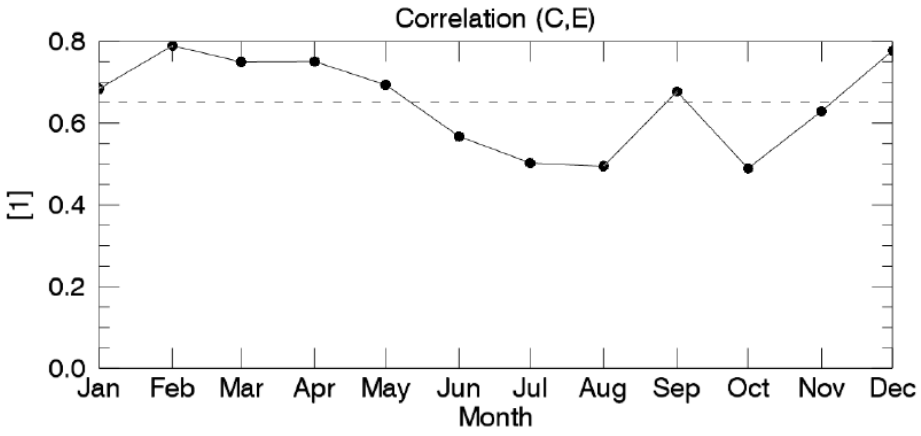

Figure 1.9: Average monthly snowfall rate (mm SWE) correlations over the Greenland Ice Sheet between CloudSat and ERA-Interim (2007-2016) (Bennartz et al., 2019).

The main scientific questions to be addressed in this thesis:

1. What are the appropriate spatial and temporal scales necessary for deriving high quality estimates of snow accumulation from CloudSat overpasses?
2. Does the performance of CloudSat snow retrievals vary in space and/or time?
3. Can CloudSat adequately capture observed climatological means and seasonality of Arctic snow accumulation?

1.4 Thesis Structure

The focus of the introduction is to provide background and motivational information related to the work described in the manuscript portion of the report, which is in chapter 2. The manuscript evaluates the extent to which CloudSat estimates of snowfall can be used to extract accurate snowfall accumulation information (Using CloudSat-CPR retrievals to estimate snow accumulation in the Canadian Arctic). The final section of this report describes the main findings, as well as the conclusions from this study, and suggests potential next steps to be taken based on the results of this research.

Chapter 2

Using CloudSat-CPR retrievals to estimate snow accumulation in the Canadian Arctic

2.1 Overview

Snow is a critical contributor to our global water and energy budget, with profound impacts for water resource availability, snow albedo feedback and flooding in cold regions. The vast size and remote nature of the Arctic present serious logistical and financial challenges to measuring snow over extended time periods. Satellite observations provided by the Cloud Profiling Radar (CPR) instrument—installed on the NASA satellite CloudSat—allow the retrieval of snowfall rates in high latitude regions, which have been used to estimate sur-

face snow accumulation. In this study, a validation of CloudSat-derived terrestrial snow estimates is presented at four Environment and Climate Change Canada (ECCC) weather stations situated in the Arctic for the common period 2007-2015. Comparisons of monthly climatological snow accumulation show mean biases of less than 1.5 mm SWE annually. Monthly time series exhibit correlations above 0.5 and RMSE below 10 mm SWE at the two highest latitude stations (Eureka and Resolute Bay) with correlations falling below 0.5 south of 70° N. CloudSat was also found to underestimate annual mean snow accumulation at the majority of sites, suggesting a potential negative bias in CloudSat's snowfall estimates, or underestimation related to sampling. These results imply that CloudSat can provide reliable estimates of snow accumulation across similar high latitude regions above 70° N. Accurate space-based snowfall measurements provide new important observational perspectives of Arctic snow accumulation, which is a critical region for environmental monitoring in an era of global change.

2.2 Introduction

Snow in the Arctic is critical to the hydrologic cycle and energy budget of the region, and through climate feedbacks this has important knock-on effects across the Northern Hemisphere, and even globally (Bokhorst et al., 2016; Brown et al., 2003; Déry and Brown, 2007). Understanding the impact of climate change on Arctic snow is, therefore, of critical importance, and is made more urgent by observed accelerated warming in high latitude regions in recent years (Bromwich et al., 2013; Church et al., 2013; Brown and Mote, 2009). In situ snow observations above 70° N are only available from approximately 21 of 1735 weather

stations across Canada (Mekis et al., 2018). These stations provide near-continuous observational records of climate parameters such as precipitation (quantity and type), and ground temperature (ECCC, 2017). Station data has been used effectively to track changes in snow accumulation at other high latitude locations in Canada as described in Derksen et al. (2003), however it can be susceptible to issues with blowing snow, phase identification and includes uncertainty introduced from the decisions and assumptions made in the processing of instrumental observations (Mekis et al., 2018). The expensive operational and maintenance costs required to keep weather stations running across an area as large and remote as the Canadian Arctic results in sparse data coverage and poor sampling throughout the region (Derksen and Brown, 2012; Liston, 2004).

Another option for estimating snow accumulation are reanalysis systems, which comprise a numerical model constrained by available observations to provide complete spatio-temporal coverage. Some commonly used reanalysis products for snow are MERRA-2, GlobSnow and CROCUS (Gelaro et al., 2017; Takala et al., 2011; Brun et al., 2012). Differences between these products relate mainly to the details of the underlying modelling system, and it can be challenging to evaluate which of a collection of similar reanalyses is the "best". For this reason, a useful approach has been to combine a series of reanalysis products together through averaging, or "blending", in an effort to increase the signal-to-noise ratio, much like the approach used in ensemble numerical weather prediction (Molteni et al., 1996).

One such product is Blended-4, which is calculated as the mean of daily gridded SWE across the Northern Hemisphere from MERRA-2, GlobSnow, CROCUS and the Simple Snow Model produced by Ross Brown (Mudryk et al., 2015; Brown and Brasnett, 2010).

The Arctic System Reanalysis (ASR) is another high-resolution reanalysis product that is primarily focused on Arctic observations and their assimilation (Bromwich et al., 2016). Both version 1 (ASRV1) and version 2 (ASRV2) of this product provide 3-hourly, high resolution land surface estimates of SWE, which are generated using the Polar Weather Forecast Model in combination with 3D-Var assimilation using the High Resolution Land Data Assimilation System (HRLDAS) scheme (Chen et al., 2007). These products can provide information on snow accumulation in high latitude regions, but are often limited by coarse spatial resolutions and relatively few available observational constraints (Kushner et al., 2018; Lindsay et al., 2014; Mudryk et al., 2015).

Remote sensing has great potential for collecting estimates of snow accumulation across the Arctic, as it can provide excellent spatial coverage with year-round sampling. The cloud-profiling radar onboard the NASA CloudSat satellite generates vertical reflectivity profiles of a cloud's inner structure (Stephens et al., 2002). Derived data products from CloudSat can be used in the classification of precipitation to identify areas of hydrometeor content within a cloud and provide estimates of surface snowfall rates that agree closely with in situ when sufficiently aggregated at high latitudes (Behrangi et al., 2016; Tanelli et al., 2008; Matrosov et al., 2008). CloudSat is especially suited for monitoring high latitude regions at monthly timescales due to the nature of its 16-day repeating orbit which can provide up to 25 instantaneous cloud measurements per month at 80° N (Fig. 2.1.a). However, sampling can be an issue when moving to lower latitudes as orbital granule tracks become less concentrated over a region resulting in fewer total observations compared to similarly sized grid cells at higher latitudes (Hiley et al., 2010). The effect of CloudSat's orbit on overpass quantity is highlighted by the difference in monthly overpass counts for

two stations (Eureka and Cambridge Bay) over 10 degrees latitude in Fig. 2.1.b.

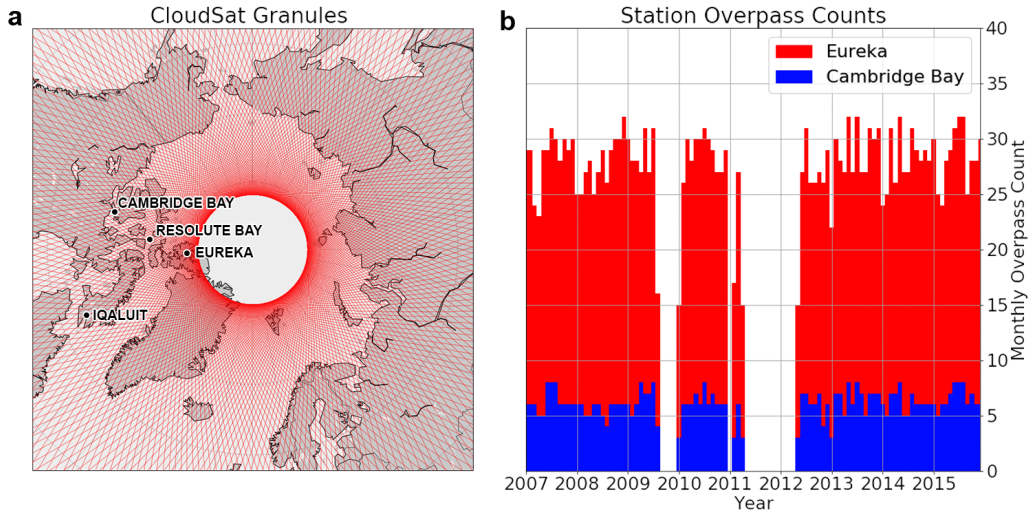

Figure 2.1: (a) 16 day repeat cycle of CloudSat orbital granule tracks over the Northern Hemisphere. (b) Stacked time series of total monthly overpass counts in a 1° grid box around Eureka (red) and Cambridge Bay (blue).

To our knowledge, a validation of CloudSat snowfall estimates against in situ snow accumulation observations from stations across the Canadian Arctic (spanning 63° N to 80° N) over the full data record of available CloudSat measurements (2007-2015), has yet to be completed. Yet, these comparisons are critical to evaluate whether CloudSat can be used to provide Pan-Arctic estimates of snowfall accumulation.

The primary goals of this thesis are to:

1. Identify the spatial and temporal scales required for obtaining a sufficiently large number of CPR samples for comparison across the Arctic

2. Compare derived CloudSat snow accumulation estimates with station data to determine whether CloudSat is a reliable source for monitoring snowfall across the Arctic

3. Examine the agreement between CloudSat and reanalysis system estimates of snow accumulation by investigating their correlations, RMSE and bias

2.3 Data and Methods

2.3.1 CloudSat Data

The CPR installed on CloudSat is a nadir-looking 94 GHz frequency (W-band) radar that measures the power backscattered from cloud particles to identify the presence of hydrometeors within a cloud (Stephens et al., 2002; Hudak et al., 2008). CloudSat's CPR observes the lowest 30 kilometers of the atmosphere divided into 125 layers (bins) of 240 meters in depth, with a 1.7 km by 1.3 km ground footprint (Palerme et al., 2014). The lowest bins of the profile, up to an altitude of 1440 meters above the surface, are contained within a radar "blind zone" where CloudSat is unable to discern meaningful observations due to interference from terrain backscatter (Milani et al., 2018). In order to derive an estimate of surface snowfall, CloudSat makes use of a "Near Surface Bin" (NSB) which is the lowest precipitating layer outside of the blind zone in the vertical cloud profile (Li L., 2007). The snowfall rate from this NSB is extrapolated down from the cloud to the terrain below which is then used to provide an estimate of the surface snowfall rate at that point directly beneath the cloud (Wood and L'Ecuyer, 2013). This NSB extrapolation can be seen in a reflectivity profile (Fig. 2.2.a) retrieved from a CloudSat overpass near Eureka station, which is used in the generation of interior cloud snowfall rates (Fig. 2.2.b) and surface snowfall rates (Fig. 2.2.c).

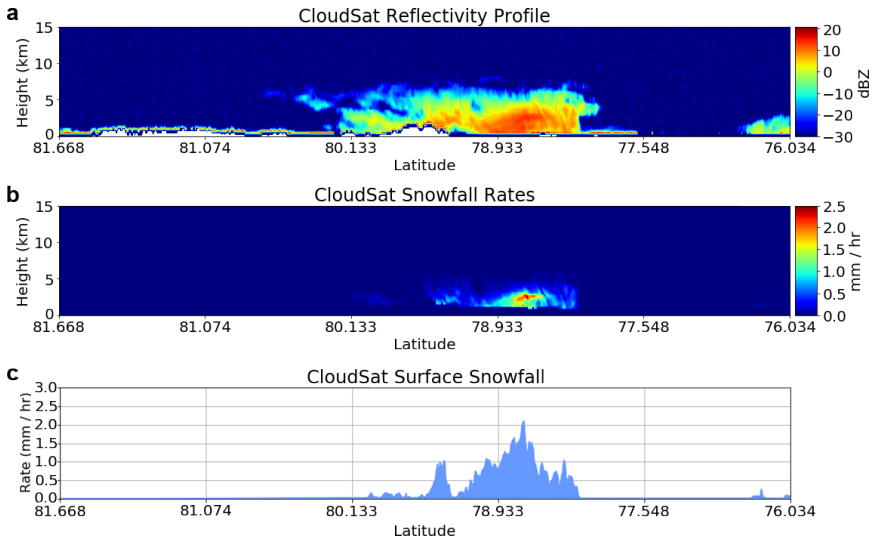

Figure 2.2: (a) Reflectivity profile derived in 2B-GEOPROF showing the power backscattered by the cloud to the CPR. (b) Vertical profile of the snowfall rate estimates in the cloud from 2C-SNOW-PROFILE. (c) Surface snowfall rates extrapolated down from the lowest precipitating cloud layer shown in (b).

The 2C-SNOW-PROFILE product, provides estimates of snowfall rates within the cloud and on the surface. This product has been examined in previous studies for Antarctica as described in Milani et al. (2018) and Palerme et al. (2014), however to our knowledge a comprehensive comparison between CloudSat, in situ station observations and reanalysis spanning the complete CloudSat record has yet to be completed over the Canadian Arctic. The CloudSat data record is available from February 2006 - August 2016, but contains a series of gaps due to battery failures that resulted in a break in CPR measurements during September 2009 - December 2009, January 2011 and May 2011 - April 2012. These missing time periods are visible as observational gaps at both of the stations shown in Fig. 2.1.b.

Discrete CloudSat profiles of snowfall rate estimates have been shown to include Bayesian uncertainties of up to 150-250 % which exist as a result of a combination of uncertainties

in CloudSat's retrieved precipitation state, particle model parameters, fallspeed model and assumptions about cloud particle distributions (Duffy and Bennartz, 2018; Wood and L'Ecuyer, 2013). However, previous work by Hiley et al. (2010) and Palerme et al. (2014) has shown that by aggregating a representative sample of discrete CloudSat profiles along the track into an "overpass average" snowfall rate, the uncertainty is considerably reduced, and the signal-to-noise ratio is increased.

To implement this aggregation method at the stations, we first define a grid box which surrounds each station, and examine all CloudSat profiles occurring within each grid box during each month. The overpass average snowfall rate is calculated as the median snowfall rate from all profiles collected in each CloudSat overpass that passes through the box. We use the median because the mean snowfall rate can be positively biased by small groups of radar profiles containing extremely large precipitation values during an overpass, and we therefore find the median more representative of the snowfall rate across the grid box as a whole. The mean monthly snowfall rate (in mm SWE hr^{-1}) is then calculated as the mean of all overpass medians in a month. Finally, assuming a constant snowfall rate throughout the month, monthly snowfall accumulation is estimated by multiplying the mean monthly snowfall rate by the total number of hours in the month, and then multiplying this result by the land cover fraction of the grid box around each station.

2.3.2 In Situ and Reanalysis Data

To perform a validation of CloudSat estimates of snowfall, suitable reference measurements of Arctic snow for ground-truthing are required. Daily historical observations of total

precipitation, total rainfall, and 2 meter air temperature over a nine-year time period are collected from four stations operated by ECCC as described in Table 2.1 with locations displayed in Fig. 2.1.a.

Table 2.1: Summary data for the historical ECCC weather station records used in the validation of CloudSat snowfall estimates. Latitude (Lat) is measured in degrees North, Longitude (Lon) is measured in degrees East, elevation is measured in meters above sea level and TC IDs are meteorological identifiers assigned to each station by Transport Canada.

Station	Lat	Lon	Elevation	WMO ID	TC ID	Missing Days
Eureka	79.99	-85.93	10	71917	WEU	0
Resolute Bay	74.72	-94.97	67.7	71924	YRB	37
Cambridge Bay	69.11	-105.14	31.1	71925	YCB	18
Iqaluit	63.75	-68.54	33.5	71321	XFB	85

These precipitation observations are recorded at each station by an automatic precipitation weighing gauge which uses vibrating wire transducers to weigh a collection bucket each day, and in turn derive an estimate of the total daily precipitation (Mekis et al., 2018). Measurements of total daily SWE are computed at each station as the difference between total precipitation and total rainfall for each day. On days when total rainfall is missing but total precipitation is available, solid and liquid precipitation are separated using a similar method to Brown et al. (2003). Any precipitation measured on days when the daily maximum temperature (T_{max}) is equal to or below 0° C is classified as entirely snow, and any precipitation measured when $T_{max} > 5$° C is classified as entirely rain. For temperatures between 0-5° C, the rain fraction is given by f_{rain}=$T_{max}/5$, and the snow fraction is $f_{snow} = 1 - f_{rain}$.

The number of missing observations in this study is shown in Table 2.1 for all stations. Missing days appear sparsely distributed across all years with only 3 of the 432 total

station-months (108 *months* $\times$ 4 *stations*) displaying more than 10 total missing days. All non-missing daily snow accumulation values are then used to derive a mean daily snow accumulation (in mm SWE) for each of the 108 months at each station. Assuming a constant snowfall rate for all days in a month, the mean daily snow accumulation for each month is then multiplied by the number of days in that month to provide an estimate of the total monthly snow accumulation at the station.

Data from the Blended-4 SWE gridded product is regridded from 0.5° resolution to 1° resolution so that it aligns with the grid used for CloudSat overpass aggregation around each station. We experimented with varying grid sizes for this comparison and found that the 1° grid performed optimally with strong correlations and low RMSE between CloudSat and the station measurements of SWE. Since the Blended-4 product contains daily estimates of SWE on ground, monthly snow accumulation is calculated as the monthly sum of all positive differences in SWE from one day to the next: $\sum_{i=1}^{n-1} d_i \ \ \forall \ \ d > 0$ where i is the subscript for each day in a month, n is the total number of days in a month, and d is the difference in mm SWE computed as $d = SWE_{i+1} - SWE_i$ (Broxton et al., 2016a). This method does not account for melt that may have occurred between two consecutive days, but provides an estimate of accumulation (only) that can be compared with snowfall measurements from CloudSat. A similar regridding process and accumulation calculation is also performed for both ASRV1 and ASRV2.

2.4 Validation of Snowfall Estimates By CloudSat at Stations in the Canadian Arctic

2.4.1 Long-term Climatological Mean Snow Accumulation

We first examine CloudSat's ability to sample monthly climatological snow accumulation at each of the four stations. Fig. 2.3 compares the seasonal cycle of monthly climatological snow accumulation observed by each station and estimated by CloudSat in a 1° grid box. Higher accumulation is observed at all stations in SON, with reduced accumulation throughout DJF and MAM (excluding Resolute Bay), followed by low levels of accumulation during the summer in JJA. CloudSat captures the broad features of the seasonal cycle at each station, with only the southernmost station Iqaluit displaying a correlation of less than 0.5 ($r = 0.28$). In terms of mean monthly snow accumulation, all of the stations displayed similar values (less than 1.5 mm SWE difference) to that of CloudSat, excluding Iqaluit which has a difference in mean annual snow accumulation (mm SWE per month) of approximately 4 mm SWE (Fig. 2.4). Additionally, based on the 95% confidence interval from the CloudSat sample, CloudSat's results are consistent with the monthly mean accumulation reported at each station. We also note a general underestimation of approximately 50% in snow accumulation from CloudSat throughout December and January across all stations. This general underestimation in CloudSat's 2C-SNOW-PROFILE snowfall rates has been previously attributed to an inability of the satellite to capture low cumuliform snowfall occurring within CloudSat's blind zone and this may be a contributing factor here as well (Bennartz et al., 2019).

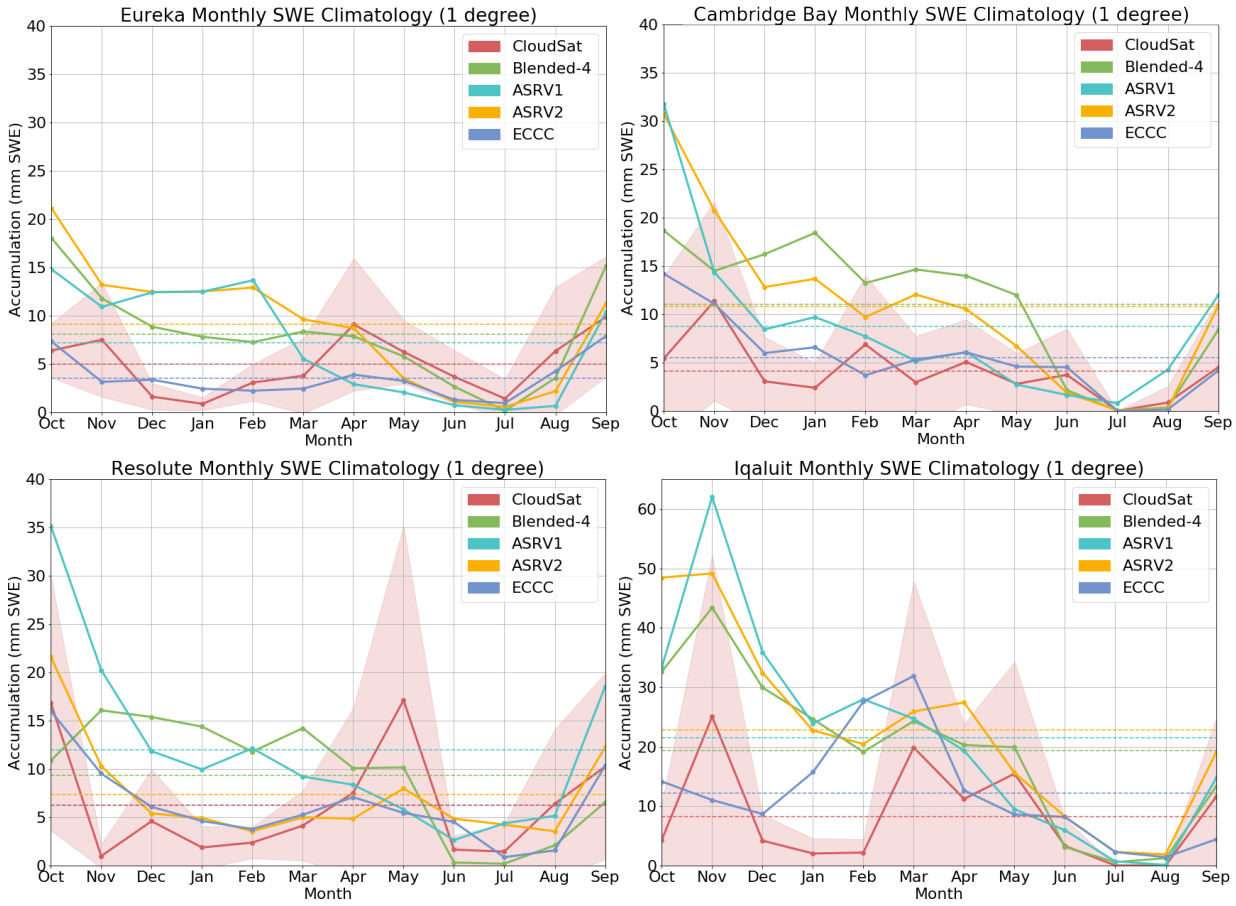

Figure 2.3: Results of the monthly snowfall accumulation climatology performed from the data retrieved in a 1 degree grid box at Eureka, Cambridge Bay, Resolute Bay and Iqaluit. The red shaded regions correspond to the 95% sampling confidence intervals from CloudSat. The mean annual snow accumulation averages (in mm per month) are displayed as colored dashed lines.

The nature of CloudSat's orbit implies that the number of overpasses at a particular ground station rapidly decreases moving towards the equator. For example, under a 1° grid, Eureka (82° N) receives on average 15-25 overpasses per month, while Iqaluit (63° N) receives just 2-3. This difference in sampling provides us with fewer observational measurements from CloudSat which results in a poorer representation of snow accumulation and declining agreement between CloudSat and station measurements moving south from 80° N. The southernmost station Iqaluit is the site showing lowest overall agreement to CloudSat, with $r = 0.28$, $RMSE = 10.9$ (mm SWE) and a bias of -3.95 (mm SWE).

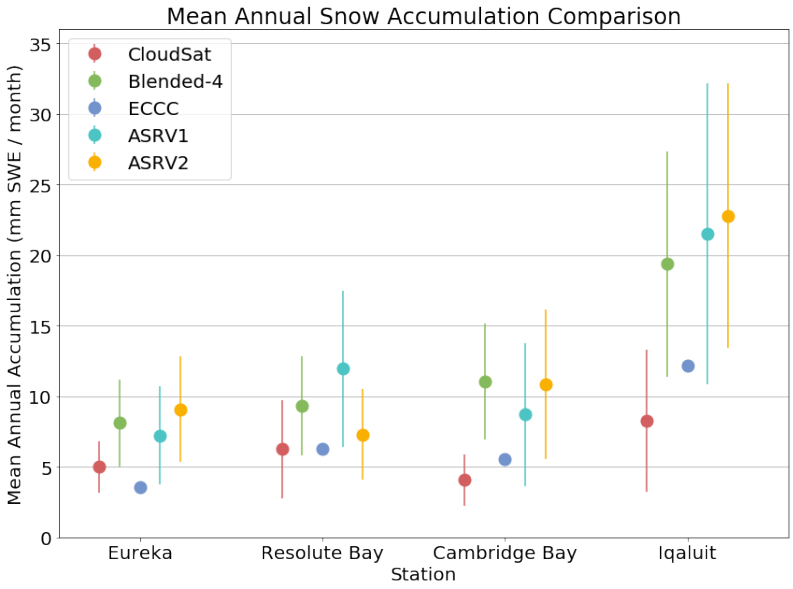

Figure 2.4: Mean annual snow accumulation (mm SWE per month) calculated for each station, CloudSat, Blended-4 and ASR. Also included are the 95% confidence intervals from the estimates provided by the CloudSat sample and gridded samples.

Turning to estimated accumulation from the different gridded SWE products, the seasonal cycle of Blended-4 is similar to CloudSat at all stations with correlations of ap-

proximately 0.5, excluding Resolute Bay ($r = 0.03$). However, Blended-4's estimates of climatological monthly mean snowfall are systematically higher than CloudSat's estimates at all stations, with the exception of the summer JJA period, where little snowfall is observed at any station. Similar seasonal cycles and climatological monthly mean snowfall values also exist between CloudSat and the ASRV2 product with correlations above 0.5 at all stations excluding Eureka ($r = 0.14$), along with low RMSE (below 10 mm SWE) at all stations excluding Iqaluit ($RMSE = 19.3$ mm SWE). We note systematically higher accumulation from both the blended product and reanalysis system estimates.

2.4.2 Interannual Variability

We next examine monthly mean estimates of snow accumulation over all 108 months in the CloudSat data record (2007-2015), which allows us to compare time series from CloudSat, ECCC and the reanalysis products. Working at a monthly time scale means that fewer CloudSat overpasses are available for each month, and so the time series display higher uncertainties and larger RMSE than the results from the climatological monthly means. We will focus on Eureka and Cambridge Bay (Fig. 2.5); Resolute Bay and Iqaluit display most of the same general features and are excluded for brevity. Overall, the performance of CloudSat at stations above 70° N (Eureka and Resolute Bay) is substantially better with higher correlations ($r = 0.79$ at Eureka) than those at lower latitudes ($r = 0.21$ at Cambridge Bay), which can again be explained by poorer temporal sampling (Table 2.2). Eureka also displays the lowest overall RMSE when compared to ECCC (5.2 mm SWE) with Cambridge Bay exhibiting increased RMSE (8.5 mm SWE) further south.

Table 2.2: Correlations and RMSE (mm SWE) of interannual variability for CloudSat (CS), ECCC (EC) and Blended-4 (B4) snow accumulation estimates at each station.

Stations	Correlation			RMSE		
	CS & EC	CS & B4	B4 & EC	CS & EC	CS & B4	B4 & EC
Eureka	0.79	0.57	0.71	5.2	7.3	6.3
Resolute Bay	0.57	0.14	0.36	9.4	12.7	8.3
Cambridge Bay	0.21	0.06	0.66	8.5	13.1	8.5
Iqaluit	0.00	0.28	0.21	31.6	25.4	24.9

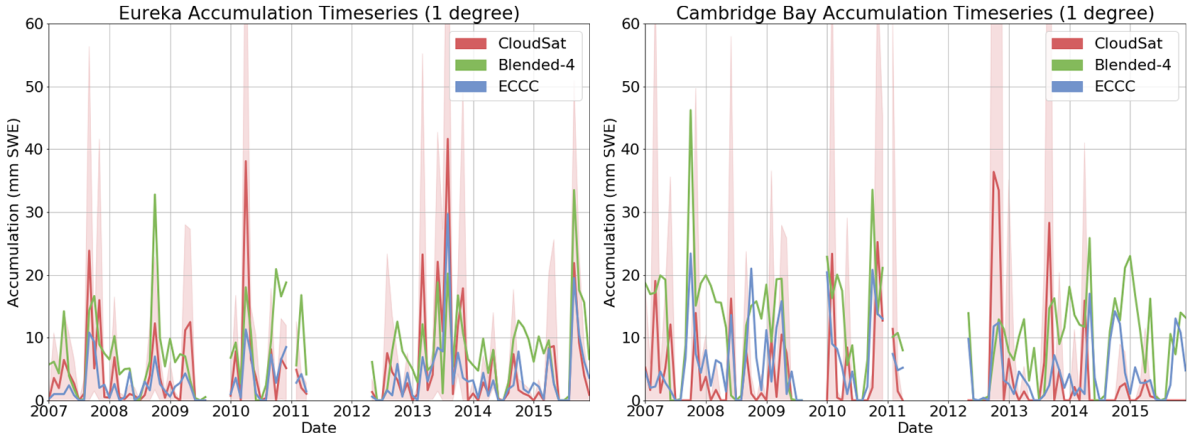

Figure 2.5: Monthly snowfall accumulation (mm SWE) time series comparisons spanning 108 months at Eureka and Cambridge Bay, with the CloudSat estimates shown in red, station estimates in blue and the Blended-4 estimates in green. The red shaded regions correspond to the 95% sampling confidence intervals from CloudSat.

These results suggest that for the approximate 5° increase in latitude between each of the stations, we find a corresponding increase in the correlation of interannual variability of at least 0.2, with the largest increase occurring between Cambridge Bay and Resolute Bay (between 69° N and 74° N). Furthermore, these results imply that there exists a southern boundary latitude, above which CloudSat observations can be used reliably to estimate monthly snow accumulation at a 1° spatial resolution near 70° N. To test whether sampling at annual (12-month) frequency could improve the sampling sufficiently to move the southern boundary, we also construct time series of annual mean snow accumulation at all stations. The annual mean results display a similar latitudinal relationship to the climatological results, with the highest correlation between CloudSat and Eureka (0.88) and the lowest at Iqaluit (-0.01). Additionally, for the stations below 70° N (Cambridge Bay and Iqaluit), moving from monthly to annual timescales still provides sample sizes that are too poor in quantity for a 1° grid to derive an estimate of snow accumulation that agrees well with in situ data.

To more clearly view inter-station similarities and differences, scatter plots of monthly snow accumulation are shown in Fig. 2.6 for Eureka and Cambridge Bay for the three pairs of data products: ECCC (EC) vs. CloudSat (CS), CloudSat vs. Blended-4 (B4), and ECCC vs Blended-4. These scatter plots of snowfall accumulation are extracted from the 108 months shown in the time series in Fig. 2.5 where the CloudSat distributions display relatively strong correlations (above 0.5) at high latitude stations ($r = 0.79$ Eureka) with lower correlations further south (0.21 at Cambridge Bay). We identified 33 out of 108 months at Cambridge Bay with zero snow accumulation in CloudSat when the corresponding value from ECCC is non-zero, compared to only nine of these months at Eureka.

This difference is again likely related to the poor temporal sampling from CloudSat at 1° resolution at these lower latitudes. With an average of only five CloudSat overpasses per month at Cambridge Bay, this appears insufficient to accurately derive estimates of monthly snow accumulation as CloudSat is missing an increased number of snowfall events occurring near the station.

Finally, we consider the comparison between CloudSat and the Blended-4 gridded product in the remaining two scatter plots of Fig. 2.6. Both Fig. 2.6.b and Fig. 2.6.c display a similar positive bias in snow accumulation in the Blended-4 estimates to what was noted in the climatology, suggesting that CloudSat's snow accumulation estimates are closer in overall magnitude to observed measurements at the station. However, Fig. 2.6.c displays a much stronger correlation between the Blended-4 and station data at Cambridge Bay ($r = 0.66$) compared to that of CloudSat and the station data ($r = 0.21$), which further highlights issues with CloudSat sampling at latitudes below 70° N.

2.5 Sources of Uncertainty in Validating CloudSat Snowfall

2.5.1 Spatial Heterogeneity

There are several highly important sources contributing to uncertainty in our evaluation of CloudSat's snow accumulation estimates. First, we have shown several times above that uncertainty due to limited temporal sampling from CloudSat becomes a critical source

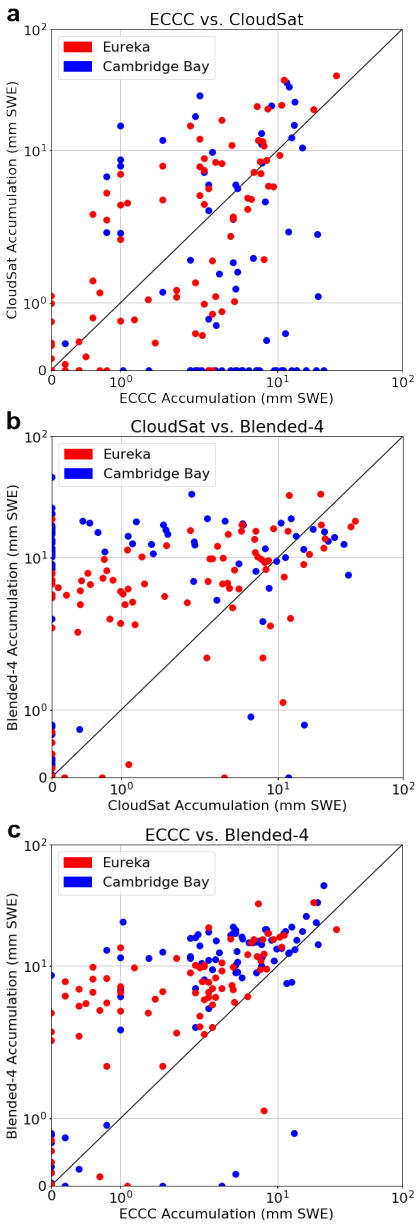

Figure 2.6: Scatter plots displaying the interannual variability of snowfall accumulation (mm SWE) for both Eureka (red) and Cambridge Bay (blue), between (a) EC and CS, (b) CS and B4, and (c) EC and B4.

of uncertainty below 70° N. Temporal averaging, through taking the climatological mean, helps to reduce the impact of sampling uncertainty (Hiley et al., 2010); however, this remains a problem at the lower-latitude stations. Furthermore, comparing aggregate estimates of snowfall from CloudSat over a grid with a point estimate at a station, provides us with additional uncertainty since observations recorded by one instrument will not necessarily be observed by the other. In order to combat this issue, we tested four spatial scales (0.5°, 1°, 1.5° and 2°) to identify the optimal grid size for use in our comparisons. Our findings indicated that the 1° grid cell was optimal as it produced results with low RMSE and high correlations when compared to the station data, and this resolution was similar to other high latitude studies using CloudSat (Palerme et al., 2017; Milani et al., 2018).

2.5.2 Snowfall Uncertainty

Additional uncertainty also arises from any near surface precipitation occurring close to a station within CloudSat's radar blind zone. The blind zone comprises the lowest 1440 m of the atmosphere where ground interference impacts the quality of CloudSat's retrievals. It has been shown in a study by Maahn et al. (2014) over a similar high latitude location in Antarctica that approximately 10% of the total annual snowfall is missed by sensors similar to those installed on CloudSat due to shallow event snowfall occurring throughout the radar blind zone (Kulie and Milani, 2018; Behrangi et al., 2016). Another recent comparison over Greenland displays similar findings from issues arising as a result of ground clutter over alpine regions influencing CPR retrievals of snowfall in the lowest precipitating bin (Bennartz et al., 2019).

Adding to uncertainties in the detection of snowfall, the CPR has a minimum detectable signal intensity of -29 dBZ which allows for the detection of light intensity precipitation, but is unable to accurately record measurements of intense precipitation due to radar signal attenuation caused by the presence of excessive ice water content, cloud liquid water, and water vapour interference (Haynes et al., 2009; Hudak et al., 2008; Kulie et al., 2010). Additionally, assumptions used by CloudSat to describe snow grain shape and particle size have been shown to be dominant contributors to modelled reflectivity (up to 4 dB) and snowfall rate uncertainties (40-60%) (Wood et al., 2013).

2.5.3 Station Measurement Uncertainties

When we consider the reference snow accumulation values from ECCC station observations, we must also consider some measurement uncertainty associated with the precipitation weighing gauges and the Data Management System (DMS) used to record and process surface weather data. There are several decisions made by the DMS in generating data records of total precipitation and the climatic assumptions used to facilitate these decisions add additional uncertainty towards each recorded measurement (Mekis et al., 2018). The precipitation weighing gauges used in the collection of total precipitation data at each of the stations are required to operate under a variety of challenging environmental conditions due to their Arctic locale. These extreme conditions can lead to problems with precipitation phase identification, bucket evaporation, precipitation accumulation on the gauge opening, and snow capping over the gauge top which can block observational records for extended time periods (Colli et al., 2015).

2.6 Conclusion

Due to the nature of CloudSat's orbit, the Arctic receives a high frequency of overpasses which results in an increased chance at observing synoptic snowfall events throughout the region. Using aggregated CloudSat profiles of snowfall rates, we are able to generate monthly estimates of snowfall accumulation from a 1° grid box over four Arctic stations. Comparing our CloudSat estimates with surface measurements from these stations allows us to identify areas of agreement, error and uncertainty. Long-term climatological CloudSat estimates of accumulated SWE display similar seasonal cycles to what is reported by the ECCC stations with strong correlations and low RMSE. Monthly CloudSat estimates at the two stations above 70° N (Eureka and Resolute Bay) performed favorably when compared with in situ data by displaying strong correlations above 0.5 and RMSE below 10 mm SWE.

As we move further south, the CloudSat overpass count begins to decline and we note decreasing correlation and increasing RMSE between monthly CloudSat estimates and station observations. When considering all four stations, we find that the highest amount of error occurs at Iqaluit, which is located at the lowest latitude and includes the fewest total number of CloudSat overpasses. These results suggest that the latitude in which CloudSat begins to perform optimally (in terms of 1° monthly correlations with ECCC station observations above 0.5 and RMSE less than 10 mm SWE), exists somewhere between Resolute Bay and Cambridge Bay where we begin to receive a minimum of approximately seven overpasses from CloudSat per month. Moving south from this location, we find the 1° grid too restrictive in terms of overpass sampling at a monthly timescale, and recommend that

a coarser resolution be considered to incorporate more overpasses into the aggregation process.

CloudSat also appears to underestimate snowfall accumulation across the Arctic with monthly and annual averages showing less accumulation compared to both the station and reanalysis. This is noted at Iqaluit, Cambridge Bay and Resolute Bay, with only Eureka displaying a higher monthly average snow accumulation estimate from CloudSat than the station observations. The differences between Eureka and the other stations may be related to the decreasing sample size as we move south, or the extreme dry conditions at Eureka combined with the fact that CloudSat has been shown to have difficulty differentiating between solid and liquid precipitation when temperatures are fluctuating near 0° C and potentially incorrectly classifying the precipitation being recorded by the ground station (Liu, 2008).

Our findings here suggest that CloudSat CPR estimates can be used as an effective perspective towards generating monthly 1° snow accumulation estimates throughout regions above 70° N. This aggregation method could therefore be generalized to a grid outside of just the four stations examined in this thesis, to provide new insights into snow accumulation throughout other Arctic regions.

Chapter 3

Conclusions

3.1 Summary

Building on similar strategies of CloudSat overpass aggregation from work by Hiley et al. (2010), Palerme et al. (2017), Milani et al. (2018), and (Bennartz et al., 2019), we find strong agreement between CloudSat and the ECCC station estimates of snow accumulation, with correlations above 0.5 and RMSE below 10 mm SWE for the northernmost stations. After experimenting with a variety of different grid boxes, we find that the 1° grid produces the necessary number of overpasses (approximately seven overpasses per month) required for achieving CloudSat and station correlations above 0.5 at monthly time scales. This lower limit of seven overpasses per month is likely also tied to the variability of snowfall for a given region, and consistently cold areas with more predictable patterns of precipitation (the cold desert conditions of Eureka) are more easily captured by CloudSat from a small

number of overpasses compared to other regions with more variability in temperature and precipitation. Northern stations performed optimally due to the increased number of CloudSat overpasses they receive, with decreasing correlations further south as the frequency of overpasses decline. CloudSat's climatological results capture the seasonality present at each location and display strong positive correlations (above 0.5) and small differences in mean monthly snow accumulation (less than 1.5 mm SWE). The effects of limited sampling at monthly time scales result in decreasing correlations (of approximately 0.2 per 5 degrees latitude) as we move south from Eureka which has the strongest overall correlation between CloudSat and ECCC ($r = 0.79$). CloudSat also performed well (with correlations above 0.5 and RMSE below 10 mm SWE) when compared to the Blended-4 dataset and reanalysis products, which display similar correlations and RMSE to that of the CloudSat and ECCC comparisons.

The critical latitude where correlations rise above 0.5 appears near 70° N (between Cambridge Bay and Resolute) where we begin to receive more then seven overpasses per month in a 1° x 1° grid box. The southernmost station Iqaluit has the lowest overall correlations between CloudSat and ECCC ($r = 0.00$) along with the largest overall RMSE of 31.6 mm SWE. Furthermore, Iqaluit receives on average 2-3 overpasses per month which is an order of magnitude less than the frequency at Eureka (15-25 overpasses per month). We also note an overall underestimation in CloudSat's estimates of snow accumulation when compared to both the ECCC and gridded estimates which is similar to the findings of other high latitude CloudSat validation studies, and may be a consequence of missing shallow cumuliform snowfall in CloudSat's observational record due to surface attenuation (Milani et al., 2018). This general underestimation is even more pronounced when we

compare the CloudSat estimates to the Blended-4 data and reanalysis products, all of which display larger estimates of accumulation compared to both CloudSat and the station observations.

The results of this validation are significant as they describe a remote sensing technique that can be used to fill current observational gaps of snow accumulation measurements across important, but difficult to observe portions of the cryosphere. As we have previously mentioned, Arctic snow is a critical contributor to our global water and energy budget with far reaching impacts to water resource availability, climate feedbacks and cold region flooding. Due to the nature of CloudSat's orbit, we have shown that the CPR presents a unique perspective in providing snow accumulation measurements across high latitude regions like the Arctic, by displaying strong correlations and low RMSE between its estimates of accumulated SWE and both in situ observations and reanalysis estimates above 70° N. Through a generalization of the techniques described here to other high latitude locations outside of the sites selected in this study, CloudSat can provide new insights into how snow is changing across Arctic regions and allow us to better prepare for and mitigate against future changes encountered under warming temperatures during an era of global change.

3.2 Future Work

The overall positive performance from CloudSat suggests that a similar method of overpass aggregation using CPR estimates could be completed over other high latitude regions to provide observational measurements of snowfall accumulation over previously difficult to

observe Arctic locale. Following the positive results of this validation over a set of high latitude locations in the Canadian Arctic, a generalization of this CloudSat overpass aggregation technique and snow accumulation estimation could be completed over other high latitude regions outside of the four grid boxes selected in this study. We have identified a range of latitudes where CPR snow data is most reliable, and it would therefore be appropriate to produce a gridded snow product over that region, which can then be compared with other gridded SWE datasets like the Blended-4 product along with its individual component members. Using the resulting CloudSat dataset, we could then provide a means to quantify potential uncertainties in reanalysis products, by providing an independent observational constraint.

Current reanalysis products and model estimates of SWE have been shown in previous studies to display biases in accumulated SWE throughout areas like the Arctic due to issues arising from model representations of ablation during periods with near-freezing temperatures (Broxton et al., 2016b). Previous literature has also shown that the poorly constrained nature of the Arctic along with the complex nature of physical snow processes occurring throughout the region can lead to increased uncertainty in reanalysis ensemble estimates of SWE (Mudryk et al., 2015). Minimizing the impacts of these limitations in current reanalysis systems would provide us with a clearer picture of how SWE is changing throughout the Arctic. The CloudSat accumulation gridded dataset would therefore an advantageous observational constraint to current gridded SWE datasets to help address known limitations in reanalysis products and provide new insights towards changes in Arctic snow.

References

Battaglia, A., Ajewole, M. O., and Simmer, C. (2007). Evaluation of radar multiple scattering effects in Cloudsat configuration. *Atmospheric Chemistry and Physics*, 7(7):1719–1730.

Beaumont, R. T. and Work, R. A. (1963). Snow Sampling Results from Three Samplers. *International Association of Scientific Hydrology. Bulletin*, 8(4):74–78.

Behrangi, A., Christensen, M., Richardson, M., Lebsock, M., Stephens, G., Huffman, G. J., Bolvin, D., Adler, R. F., Gardner, A., Lambrigtsen, B., and Fetzer, E. (2016). Status of high-latitude precipitation estimates from observations and reanalyses. *Journal of Geophysical Research: Atmospheres*, 121(9):4468–4486.

Bennartz, R., Fell, F., Pettersen, C., Shupe, M. D., and Schuettemeyer, D. (2019). Spatial and temporal variability of snowfall over Greenland from CloudSat observations. *Atmospheric Chemistry and Physics Discussions*, pages 1–32.

Boening, C., Lebsock, M., Landerer, F., and Stephens, G. (2012). Snowfall-driven mass change on the East Antarctic ice sheet. *Geophysical Research Letters*, 39(21).

Bokhorst, S., Pedersen, S. H., Brucker, L., Anisimov, O., Bjerke, J. W., Brown, R. D., Ehrich, D., Essery, R. L. H., Heilig, A., Ingvander, S., Johansson, C., Johansson, M., Jnsdttir, I. S., Inga, N., Luojus, K., Macelloni, G., Mariash, H., McLennan, D., Rosqvist, G. N., Sato, A., Savela, H., Schneebeli, M., Sokolov, A., Sokratov, S. A., Terzago, S., Vikhamar-Schuler, D., Williamson, S., Qiu, Y., and Callaghan, T. V. (2016). Changing Arctic snow cover: A review of recent developments and assessment of future needs for observations, modelling, and impacts. *Ambio*, 45(5):516–537.

Bromwich, D., Bai, L., Hines, K., Wang, S.-h., Liu, Z., Lin, H.-C., Kuo, Y.-h., and Barlage, M. (2012). Arctic System Reanalysis (ASR) Project. type: dataset.

Bromwich, D. H. and Fogt, R. L. (2004). Strong Trends in the Skill of the ERA-40 and NCEPNCAR Reanalyses in the High and Midlatitudes of the Southern Hemisphere, 19582001. *Journal of Climate*, 17(23):4603–4619.

Bromwich, D. H., Nicolas, J. P., Monaghan, A. J., Lazzara, M. A., Keller, L. M., Weidner, G. A., and Wilson, A. B. (2013). Central West Antarctica among the most rapidly warming regions on Earth. *Nature Geoscience*, 6(2):139–145.

Bromwich, D. H., Wilson, A. B., Bai, L.-S., Moore, G. W. K., and Bauer, P. (2016). A comparison of the regional Arctic System Reanalysis and the global ERA-Interim Reanalysis for the Arctic. *Quarterly Journal of the Royal Meteorological Society*, 142(695):644–658.

Brown, R. and Brasnett, B. (2010). Canadian meteorological centre (cmc) daily snow depth analysis data, version 1. *NASA National Snow and Ice Data Center Distributed Active Archive Center*.

Brown, R. D., Brasnett, B., and Robinson, D. (2003). Gridded North American monthly snow depth and snow water equivalent for GCM evaluation. *Atmosphere-Ocean*, 41(1):1–14.

Brown, R. D. and Mote, P. W. (2009). The Response of Northern Hemisphere Snow Cover to a Changing Climate. *Journal of Climate*, 22(8):2124–2145.

Broxton, P. D., Dawson, N., and Zeng, X. (2016a). Linking snowfall and snow accumulation to generate spatial maps of SWE and snow depth. *Earth and Space Science*, 3(6):246–256.

Broxton, P. D., Zeng, X., and Dawson, N. (2016b). Why Do Global Reanalyses and Land Data Assimilation Products Underestimate Snow Water Equivalent? *Journal of Hydrometeorology*, 17(11):2743–2761.

Brun, E., Vionnet, V., Boone, A., Decharme, B., Peings, Y., Valette, R., Karbou, F., and Morin, S. (2012). Simulation of Northern Eurasian Local Snow Depth, Mass, and Density Using a Detailed Snowpack Model and Meteorological Reanalyses. *Journal of Hydrometeorology*, 14(1):203–219.

Brutel-Vuilmet, C., Mngoz, M., and Krinner, G. (2013). An analysis of present and future seasonal Northern Hemisphere land snow cover simulated by CMIP5 coupled climate models. *The Cryosphere*, 7(1):67–80.

Bucholtz, A. (1995). Rayleigh-scattering calculations for the terrestrial atmosphere. *Applied Optics*, 34(15):2765–2773.

Callaghan, T. V., Johansson, M., Brown, R. D., Groisman, P. Y., Labba, N., Radionov, V., Barry, R. G., Bulygina, O. N., Essery, R. L. H., Frolov, D. M., Golubev, V. N., Grenfell, T. C., Petrushina, M. N., Razuvaev, V. N., Robinson, D. A., Romanov, P., Shindell, D., Shmakin, A. B., Sokratov, S. A., Warren, S., and Yang, D. (2011). The Changing Face of Arctic Snow Cover: A Synthesis of Observed and Projected Changes. *AMBIO*, 40(1):17–31.

Chen, F., Manning, K. W., LeMone, M. A., Trier, S. B., Alfieri, J. G., Roberts, R., Tewari, M., Niyogi, D., Horst, T. W., Oncley, S. P., Basara, J. B., and Blanken, P. D. (2007). Description and Evaluation of the Characteristics of the NCAR High-Resolution Land Data Assimilation System. *Journal of Applied Meteorology and Climatology*, 46(6):694–713.

Church, J., P.U. Clark, A. C., J.M. Gregory, S. J., A. Levermann, M. M., G.A. Milne, R. N., P.D. Nunn, A. P., W.T. Pfeffer, D. S., and Unnikrishnan, A. (2013). Sea level change. *Climate Change 2013: The Physical Science Basis. Contribution of Working Group I to the Fifth Assessment Report of the Intergovernmental Panel on Climate Change*.

Colli, M., Rasmussen, R., Thriault, J. M., Lanza, L. G., Baker, C. B., and Kochendorfer, J. (2015). An Improved Trajectory Model to Evaluate the Collection Performance of Snow Gauges. *Journal of Applied Meteorology and Climatology*, 54(8):1826–1836.

Danco, J. F., DeAngelis, A. M., Raney, B. K., and Broccoli, A. J. (2016). Effects of a Warming Climate on Daily Snowfall Events in the Northern Hemisphere. *Journal of Climate*, 29(17):6295–6318.

Dee, D. P. and Uppala, S. (2009). Variational bias correction of satellite radiance data in the ERA-Interim reanalysis. *Quarterly Journal of the Royal Meteorological Society*, 135(644):1830–1841.

Dee, D. P., Uppala, S. M., Simmons, A. J., Berrisford, P., Poli, P., Kobayashi, S., Andrae, U., Balmaseda, M. A., Balsamo, G., Bauer, P., Bechtold, P., Beljaars, A. C. M., Berg, L. v. d., Bidlot, J., Bormann, N., Delsol, C., Dragani, R., Fuentes, M., Geer, A. J., Haimberger, L., Healy, S. B., Hersbach, H., Hlm, E. V., Isaksen, L., Kllberg, P., Khler, M., Matricardi, M., McNally, A. P., MongeSanz, B. M., Morcrette, J.-J., Park, B.-K., Peubey, C., Rosnay, P. d., Tavolato, C., Thpaut, J.-N., and Vitart, F. (2011). The ERA-Interim reanalysis: configuration and performance of the data assimilation system. *Quarterly Journal of the Royal Meteorological Society*, 137(656):553–597.

Derksen, C. and Brown, R. (2012). Spring snow cover extent reductions in the 20082012 period exceeding climate model projections. *Geophysical Research Letters*, 39(19).

Derksen, C., Walker, A., and Goodison, B. (2003). A comparison of 18 winter seasons of in situ and passive microwave-derived snow water equivalent estimates in Western Canada. *Remote Sensing of Environment*, 88(3):271–282.

Déry, S. J. and Brown, R. D. (2007). Recent Northern Hemisphere snow cover extent trends and implications for the snow-albedo feedback. *Geophysical Research Letters*, 34(22).

Dietz, A. J., Kuenzer, C., Gessner, U., and Dech, S. (2012). Remote sensing of snow: a review of available methods. *International Journal of Remote Sensing*, 33(13):4094–4134.

Doesken, N. J. and Robinson, D. A. (2009). The Challenge of Snow Measurements. In Dupigny-Giroux, L.-A. and Mock, C. J., editors, *Historical Climate Variability and Impacts in North America*, pages 251–273. Springer Netherlands, Dordrecht.

Dozier, J. (1989). Spectral signature of alpine snow cover from the landsat thematic mapper. *Remote Sensing of Environment*, 28:9–22.

Duffy, G. and Bennartz, R. (2018). The Role of Melting Snow in the Ocean Surface Heat Budget. *Geophysical Research Letters*, 45(18):9782–9789.

ECCC (2017). Technical documentation - digital archive of canadian climatological data. *Environment and Climate Change Canada Documentation*, page 35.

Fountain, A. G., Nylen, T. H., Monaghan, A., Basagic, H. J., and Bromwich, D. (2009). Snow in the McMurdo Dry Valleys, Antarctica. *International Journal of Climatology*, pages n/a–n/a.

Frei, A. and Robinson, D. A. (1998). Evaluation of snow extent and its variability in the Atmospheric Model Intercomparison Project. *Journal of Geophysical Research: Atmospheres*, 103(D8):8859–8871.

Gelaro, R., McCarty, W., Surez, M. J., Todling, R., Molod, A., Takacs, L., Randles, C. A., Darmenov, A., Bosilovich, M. G., Reichle, R., Wargan, K., Coy, L., Cullather, R., Draper, C., Akella, S., Buchard, V., Conaty, A., da Silva, A. M., Gu, W., Kim, G.-K., Koster, R., Lucchesi, R., Merkova, D., Nielsen, J. E., Partyka, G., Pawson, S., Putman, W., Rienecker, M., Schubert, S. D., Sienkiewicz, M., and Zhao, B. (2017). The

Modern-Era Retrospective Analysis for Research and Applications, Version 2 (MERRA-2). *Journal of Climate*, 30(14):5419–5454.

Genthon, C., Krinner, G., and Castebrunet, H. (2009). Antarctic precipitation and climate-change predictions: horizontal resolution and margin vs plateau issues. *Annals of Glaciology*, 50(50):55–60.

Hall, D. (2012). *Remote Sensing of Ice and Snow*. Springer Science & Business Media. Google-Books-ID: mt0sBAAAQBAJ.

Haynes, J. M., L'Ecuyer, T. S., Stephens, G. L., Miller, S. D., Mitrescu, C., Wood, N. B., and Tanelli, S. (2009). Rainfall retrieval over the ocean with spaceborne W-band radar. *Journal of Geophysical Research: Atmospheres*, 114(D8).

Hiley, M. J., Kulie, M. S., and Bennartz, R. (2010). Uncertainty Analysis for CloudSat Snowfall Retrievals. *Journal of Applied Meteorology and Climatology*, 50(2):399–418.

Hou, A. Y., Kakar, R. K., Neeck, S., Azarbarzin, A. A., Kummerow, C. D., Kojima, M., Oki, R., Nakamura, K., and Iguchi, T. (2014). The Global Precipitation Measurement Mission. *Bulletin of the American Meteorological Society*, 95(5):701–+. WOS:000339091500008.

Hudak, D., Rodriguez, P., and Donaldson, N. (2008). Validation of the CloudSat precipitation occurrence algorithm using the Canadian C band radar network. *Journal of Geophysical Research: Atmospheres*, 113(D8):D00A07.

Kochendorfer, J., Rasmussen, R., Wolff, M., Baker, B., Hall, M. E., Meyers, T., Landolt, S., Jachcik, A., Isaksen, K., Brkkan, R., and Leeper, R. (2017). The quantification

and correction of wind-induced precipitation measurement errors. *Hydrology and Earth System Sciences*, 21(4):1973–1989.

Kulie, M. S. and Bennartz, R. (2009). Utilizing Spaceborne Radars to Retrieve Dry Snowfall. *Journal of Applied Meteorology and Climatology*, 48(12):2564–2580.

Kulie, M. S., Bennartz, R., Greenwald, T. J., Chen, Y., and Weng, F. (2010). Uncertainties in Microwave Properties of Frozen Precipitation: Implications for Remote Sensing and Data Assimilation. *Journal of the Atmospheric Sciences*, 67(11):3471–3487.

Kulie, M. S. and Milani, L. (2018). Seasonal variability of shallow cumuliform snowfall: A CloudSat perspective. *Quarterly Journal of the Royal Meteorological Society*, 144(S1):329–343.

Kushner, P. J., Mudryk, L. R., Merryfield, W., Ambadan, J. T., Berg, A., Bichet, A., Brown, R., Derksen, C., Dery, S. J., Dirkson, A., Flato, G., Fletcher, C. G., Fyfe, J. C., Gillet, N., Haas, C., Howell, S., Laliberte, F., McCusker, K., Sigmond, M., Sospedra-Alfonso, R., Tandon, N. F., Thackeray, C., Tremblay, B., and Zwiers, F. W. (2018). Canadian snow and sea ice: assessment of snow, sea ice, and related climate processes in Canadas Earth system model and climate-prediction system. *The Cryosphere*, 12:1137–1156.

Li L., Durden S., T. S. (2007). Level 1 b cpr process description and interface control document. *Jet Propulsion Laboratory*, page 24.

Lindsay, R., Wensnahan, M., Schweiger, A., and Zhang, J. (2014). Evaluation of Seven Dif-

ferent Atmospheric Reanalysis Products in the Arctic. *Journal of Climate*, 27(7):2588–2606.

Liston, G. E. (2004). Representing Subgrid Snow Cover Heterogeneities in Regional and Global Models. *Journal of Climate*, 17(6):1381–1397.

Liu, G. (2008). Deriving snow cloud characteristics from CloudSat observations. *Journal of Geophysical Research: Atmospheres*, 113(D8):D00A09.

Lorenc, A. C. (1986). Analysis methods for numerical weather prediction. *Quarterly Journal of the Royal Meteorological Society*, 112(474):1177–1194.

Maahn, M., Burgard, C., Crewell, S., Gorodetskaya, I. V., Kneifel, S., Lhermitte, S., Tricht, K. V., and Lipzig, N. P. M. v. (2014). How does the spaceborne radar blind zone affect derived surface snowfall statistics in polar regions? *Journal of Geophysical Research: Atmospheres*, 119(24):13,604–13,620.

Marchand, R., Mace, G. G., Ackerman, T., and Stephens, G. (2008). Hydrometeor Detection Using CloudsatAn Earth-Orbiting 94-GHz Cloud Radar. *Journal of Atmospheric and Oceanic Technology*, 25(4):519–533.

Marks, D., Cooley, K. R., Robertson, D. C., and Winstral, A. (2018). Long-Term Snow Database, Reynolds Creek Experimental Watershed, Idaho, United States. *Water Resources Research*, pages 2835–2838.

Marzano, F. S., Roberti, L., Michele, S. D., Mugnai, A., and Tassa, A. (2003). Modeling of apparent radar reflectivity due to convective clouds at attenuating wavelengths. *Radio Science*, 38(1):2–1–2–16.

Matrosov, S. Y., Shupe, M. D., and Djalalova, I. V. (2008). Snowfall Retrievals Using Millimeter-Wavelength Cloud Radars. *Journal of Applied Meteorology and Climatology*, 47(3):769–777.

Matsui, T., Iguchi, T., Li, X., Han, M., Tao, W.-K., Petersen, W., L'Ecuyer, T., Meneghini, R., Olson, W., Kummerow, C. D., Hou, A. Y., Schwaller, M. R., Stocker, E. F., and Kwiatkowski, J. (2013). GPM Satellite Simulator over Ground Validation Sites. *Bulletin of the American Meteorological Society*, 94(11):1653–1660.

McKay, D. C. and Thurtell, G. W. (1978). Measurements of the Energy Fluxes Involved in the Energy Budget of a Snow Cover. *Journal of Applied Meteorology*, 17(3):339–349.

Mekis, E., Donaldson, N., Reid, J., Zucconi, A., Hoover, J., Li, Q., Nitu, R., and Melo, S. (2018). An Overview of Surface-Based Precipitation Observations at Environment and Climate Change Canada. *Atmosphere-Ocean*, 56(2):71–95.

Milani, L., Kulie, M. S., Casella, D., Dietrich, S., L'Ecuyer, T. S., Panegrossi, G., Porc, F., San, P., and Wood, N. B. (2018). CloudSat snowfall estimates over Antarctica and the Southern Ocean: An assessment of independent retrieval methodologies and multi-year snowfall analysis. *Atmospheric Research*, 213:121–135.

Molteni, F., Buizza, R., Palmer, T. N., and Petroliagis, T. (1996). The ECMWF Ensemble Prediction System: Methodology and validation. *Quarterly Journal of the Royal Meteorological Society*, 122(529):73–119.

Mudryk, L. R., Derksen, C., Kushner, P. J., and Brown, R. (2015). Characterization of

Northern Hemisphere Snow Water Equivalent Datasets, 19812010. *Journal of Climate*, 28(20):8037–8051.

Palerme, C., Claud, C., Dufour, A., Genthon, C., Wood, N. B., and L'Ecuyer, T. (2017). Evaluation of Antarctic snowfall in global meteorological reanalyses. *Atmospheric Research*, 190:104–112.

Palerme, C., Kay, J. E., Genthon, C., L'Ecuyer, T., Wood, N. B., and Claud, C. (2014). How much snow falls on the Antarctic ice sheet? *The Cryosphere*, 8(4):1577–1587.

Parker, W. S. (2016). Reanalyses and Observations: Whats the Difference? *Bulletin of the American Meteorological Society*, 97(9):1565–1572.

Peacock, S. (2012). Projected Twenty-First-Century Changes in Temperature, Precipitation, and Snow Cover over North America in CCSM4. *Journal of Climate*, 25(13):4405–4429.

Rienecker, M. M., Suarez, M. J., Gelaro, R., Todling, R., Bacmeister, J., Liu, E., Bosilovich, M. G., Schubert, S. D., Takacs, L., Kim, G.-K., Bloom, S., Chen, J., Collins, D., Conaty, A., da Silva, A., Gu, W., Joiner, J., Koster, R. D., Lucchesi, R., Molod, A., Owens, T., Pawson, S., Pegion, P., Redder, C. R., Reichle, R., Robertson, F. R., Ruddick, A. G., Sienkiewicz, M., and Woollen, J. (2011a). MERRA: NASAs Modern-Era Retrospective Analysis for Research and Applications. *Journal of Climate*, 24(14):3624–3648.

Rienecker, M. M., Suarez, M. J., Gelaro, R., Todling, R., Bacmeister, J., Liu, E., Bosilovich, M. G., Schubert, S. D., Takacs, L., Kim, G.-K., Bloom, S., Chen, J., Collins, D., Conaty, A., da Silva, A., Gu, W., Joiner, J., Koster, R. D., Lucchesi, R., Molod, A., Owens, T.,

Pawson, S., Pegion, P., Redder, C. R., Reichle, R., Robertson, F. R., Ruddick, A. G., Sienkiewicz, M., and Woollen, J. (2011b). MERRA: NASAs Modern-Era Retrospective Analysis for Research and Applications. *Journal of Climate*, 24(14):3624–3648.

Risnen, J. (2008). Warmer climate: less or more snow? *Climate Dynamics*, 30(2):307–319.

Serreze, M. C. and Barry, R. G. (2011). Processes and impacts of Arctic amplification: A research synthesis. *Global and Planetary Change*, 77(1):85–96.

Smith, C. D. (2009). Correcting the wind bias in snowfall measurements made with a geonor t-200b precipitation gauge and alter wind shield. *Western Snow Conference*, pages 115–121.

Souverijns, N., Gossart, A., Lhermitte, S., Gorodetskaya, I. V., Grazioli, J., Berne, A., Duran-Alarcon, C., Boudevillain, B., Genthon, C., Scarchilli, C., and van Lipzig, N. P. M. (2018). Evaluation of the CloudSat surface snowfall product over Antarctica using ground-based precipitation radars. *The Cryosphere Discussions*, pages 1–21.

Steiner, L., Meindl, M., Fierz, C., and Geiger, A. (2018). An assessment of sub-snow GPS for quantification of snow water equivalent. *Cryosphere*, 12(10):3161–3175. WOS:000446326400002.

Stephens, G. L., Vane, D. G., Boain, R. J., Mace, G. G., Sassen, K., Wang, Z., Illingworth, A. J., O'connor, E. J., Rossow, W. B., Durden, S. L., Miller, S. D., Austin, R. T., Benedetti, A., and Mitrescu, C. (2002). The cloudsat mission and the a-train. *Bulletin of the American Meteorological Society*, 83(12):1771–1790.

Takala, M., Luojus, K., Pulliainen, J., Derksen, C., Lemmetyinen, J., Krn, J.-P., Koskinen, J., and Bojkov, B. (2011). Estimating northern hemisphere snow water equivalent for climate research through assimilation of space-borne radiometer data and ground-based measurements. *Remote Sensing of Environment*, 115(12):3517–3529.

Tanelli, S., Durden, S. L., Im, E., Pak, K. S., Reinke, D. G., Partain, P., Haynes, J. M., and Marchand, R. T. (2008). CloudSat's Cloud Profiling Radar After Two Years in Orbit: Performance, Calibration, and Processing. *IEEE Transactions on Geoscience and Remote Sensing*, 46(11):3560–3573.

UCAR/NCAR, O.-S. (2017). Arctic System Reanalysis version 2. type: dataset.

Vavrus, S. (2007). The role of terrestrial snow cover in the climate system. *Climate Dynamics*, 29(1):73–88. WOS:000246520800006.

Winther, J.-G., Gerland, S., rbk, J. B., Ivanov, B., Blanco, A., and Boike, J. (1999). Spectral reflectance of melting snow in a high Arctic watershed on Svalbard: some implications for optical satellite remote sensing studies. *Hydrological Processes*, 13(12-13):2033–2049.

Woo, M.-k., Heron, R., Marsh, P., and Steer, P. (1983). Comparison of weather station snowfall with winter snow accumulation in high arctic basins. *Atmosphere-Ocean*, 21(3):312–325.

Wood, N. B. and L'Ecuyer, T. S. (2013). Level 2c snow-profile process description and interface control document, product version p1_r05. *NASA JPL CloudSat project document revision*, page 26.

Wood, N. B., L'Ecuyer, T. S., Bliven, F. L., and Stephens, G. L. (2013). Characterization of video disdrometer uncertainties and impacts on estimates of snowfall rate and radar reflectivity. *Atmospheric Measurement Techniques*, 6(12):3635–3648.

Wood, N. B., L'Ecuyer, T. S., Heymsfield, A. J., Stephens, G. L., Hudak, D. R., and Rodriguez, P. (2014). Estimating snow microphysical properties using collocated multisensor observations. *Journal of Geophysical Research: Atmospheres*, 119(14):8941–8961.